



In vitro anticancer active *cis*-Pt(II)-diiodido complexes containing 4-azaindoles

Pavel Štarha¹ · Zdeněk Trávníček¹ · Ján Vančo¹ · Zdeněk Dvořák¹

Received: 1 November 2018 / Accepted: 27 December 2018
© Society for Biological Inorganic Chemistry (SBIC) 2019

Abstract

4-Azaindole (1*H*-pyrrolo[3,2-*b*]pyridine; 4aza) and its *N*1-alkylated derivative *N*1-isopropyl-4-azaindole (1-(propan-2-yl)-1*H*-pyrrolo[3,2-*b*]pyridine; *ip*4aza) have been used for the preparation of the *cis*-diiodido-platinum(II) complexes *cis*-[Pt(4aza)₂I₂] (**1**), *cis*-[PtI₂(*ip*4aza)₂] (**2**), *cis*-[Pt(4aza)I₂(NH₃)] (**3**) and *cis*-[PtI₂(*ip*4aza)(NH₃)] (**4**). The prepared complexes were thoroughly characterized (e.g., multinuclear NMR spectroscopy and ESI mass spectrometry) and their in vitro cytotoxicity was assessed at human ovarian carcinoma (A2780), cisplatin-resistant ovarian carcinoma (A2780R) and colon carcinoma (HT-29) cell lines, where they showed, in some cases, significantly higher activity than the used reference-drug cisplatin. The results of in vitro cytotoxicity testing at the A2780 and A2780R cells indicated that alkylation of the 4-azaindole moiety at the position of the *N*1 atom had a positive biological effect, because the *ip*4aza-containing complexes **2** and **4** showed significantly ($p < 0.005$) higher cytotoxicity than 4aza-containing analogues **1** and **3**. The resistance factors (A2780R/A2780 model) equalled 0.8–1.4, indicating the ability of complexes **1–4** to overcome the acquired resistance of the A2780 cells against cisplatin. Complexes **1** and **2** revealed low toxicity against primary culture of human hepatocytes. The flow cytometry studies of the A2780 cell cycle modification showed that complexes **1–4** induce different cell cycle perturbations as compared with cisplatin, thus suggesting a different mechanism of their antitumor action.

Keywords Platinum(II) complexes · 4-Azaindole · Iodido · Cytotoxicity · In vitro

Introduction

Several platinum(II) complexes are clinically used for the treatment of various cancer types [1]. Among them, the *cis*-diammine-dichloridoplatinum(II) complex (cisplatin, *cis*-[PtCl₂(NH₃)₂]) [2], approved in 1978 by FDA for the clinical use, still represents the crucial anticancer drug applied for the treatment of cancer patients receiving chemotherapy [3]. Besides the clinical use of the platinum-based drugs [1], topicality and perspective of development and bioanalysis of novel platinum(II) complexes are underlined by several

pharmacologically prospective representatives reported in the literature in past few years [4], such as *phenanthriplatin* ([PtCl(NH₃)₂(Ph)]Cl; Ph = phenanthridine) [5]. However, it has to be stated here that it is not only platinum, whose complexes have been studied for their anticancer activity, because there is a plenty of other platinum-group metal complexes [e.g., 6, 7] or other transition metal complexes [8, 9], which have been recently reported as highly cytotoxic and prospective from the pharmacological point of view.

In general, 7-azaindoles are frequently used as suitable *N*-donor ligand for various types of complexes of many transition metals [10]. To date, several research teams have been dealt with platinum(II) complexes containing 7-azaindole (1*H*-pyrrolo[2,3-*b*]pyridine) and its *C*- or *N*-derivatives (7aza) as *N*-donor carrier-ligands [11–19]. Some concrete examples of such complexes which have been prepared and bioanalysed in last couple of years are as follows: *cis*-[Pt(7aza)₂Cl₂] [11–13], *cis/trans*-[Pt(7aza)Cl₂(NH₃)] [14, 15], [Pt(7aza)₂(cbdc)] [16], [Pt(7aza)₂(ox)] [17], [Pt(7aza)₂(mal)] and *cis*-[Pt(7aza)₂(dec)₂] [18], and *cis*-[Pt(7aza)₂I₂] [19]; cbdc = cyclobutane-1,1-dicarboxylato,

Electronic supplementary material The online version of this article (<https://doi.org/10.1007/s00775-019-01643-8>) contains supplementary material, which is available to authorized users.

✉ Zdeněk Trávníček
zdenek.travnicek@upol.cz

¹ Biologically Active Complexes and Molecular Magnets, Regional Centre of Advanced Technologies and Materials, Faculty of Science, Palacký University in Olomouc, Šlechtitelů 27, 783 71 Olomouc, Czech Republic

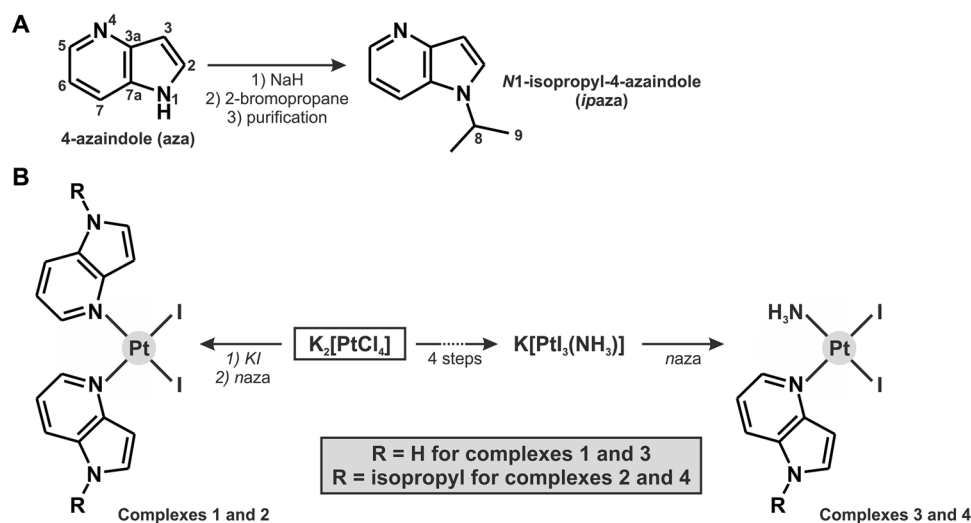
ox = oxalato, dec = decanoato and mal = malonato. Among them, the *cis*-[PtCl₂(7aza)₂] complexes showed considerably higher in vitro cytotoxicity against a panel of human cancer cell lines than cisplatin [13, 20, 21], high anticancer activity in vivo [20] and relevant differences in several processes connected with their mechanism of action as compared with cisplatin [13, 20, 22]. However, in vitro cytotoxicity of the mentioned *cis*-[Pt(7aza)₂Cl₂] complexes was in many cases surpassed by their diiodido analogues. For example, the best-performing chlorido complex *cis*-[Pt(7aza¹)₂Cl₂] (7aza¹ = 4-bromo-7-azaindole) was highly effective against the human A2780 ovarian carcinoma, HOS osteosarcoma, MCF7 breast carcinoma and HeLa cervix carcinoma cell lines, with RA ~ 5.7, 5.6, 6.7 and 4.3, respectively [21]; RA (relative activity) = IC₅₀(cisplatin)/IC₅₀(complex). However, the RA values obtained for the analogical diiodido complex *cis*-[Pt(7aza¹)₂I₂] were markedly higher (ca. 8.8, 47.3, 17.9, and 8.0, respectively) than for the complex *cis*-[Pt(7aza¹)₂Cl₂] [19]. Furthermore, the diiodido complexes were also found to be anticancer effective in vivo and their mechanism of action seems to be different from their chlorido analogues as well as from cisplatin [23, 24].

Although complexes containing 7-azaindole or its derivatives are well known in the literature [10], 4-azaindole (1*H*-pyrrolo[3,2-*b*]pyridine; 4aza) or its derivatives (in any protonation state) have been used as ligands of transition metal complexes only in two works [25, 26]. In particular, complex *cis*-[Ru(4aza)(bpy)₂Cl]PF₆ containing electroneutral 4aza [25], and Na₂[Fe(4aza⁻)₄].2Solv (Solv = tetrahydrofuran (THF) or CH₃CN) containing deprotonated 4aza [26], have been prepared. It is also noteworthy, that variously substituted 4-azaindole derivatives exhibit high biological activity of different type, such as antitubercular activity [27, 28], p21-activated kinase inhibition activity [29], HIV-1 attachment inhibition activity [30] or cytotoxic and protein kinase inhibition activity [31].

With respect to the above-mentioned high in vitro cytotoxicity of platinum(II) complexes containing 7-azaindoles, it was of great interest to investigate whether the platinum(II) complexes containing 4-azaindoles will affect the cell viability of selected human cancer cell lines as well. Since complexes *cis*-[Pt(7aza)₂I₂] represent the most cytotoxic structural type of platinum(II) agents containing 7-azaindoles [19], we chose this structural type of compounds (i.e., diiodido complexes) for the present study as well, with the aim to find out how a relatively small structural change (i.e., N1 substitution by isopropyl) of 4aza may influence the resulting cytotoxicity of the final complexes, as it can be deduced from the literature data reported for a couple of platinum(II) dichlorido complexes *cis*-[Pt(7aza)Cl₂(NH₃)] (RA ~ 0.4) [14] and *cis*-[PtCl₂(*Me*7aza)(NH₃)] (RA ~ 0.6) [15], both studied at the A2780 cells (72 h exposure) and referenced against cisplatin; *Me*7aza = *N*1-methyl-7-azaindole (1-(methyl)-1*H*-pyrrolo[2,3-*b*]pyridine). Next motivation can be associated with the previous findings that complexes *cis*-[PtI₂(Lⁿ)(NH₃)], containing 5,7-diphenyl-1,2,4-triazolo[1,5-*a*]pyrimidine (L¹) [32] or L² = 2-(4-chlorophenyl)-8-aminoimidazo[1,2-*a*]pyridin-3-yl]-*N,N*-di-*n*-propylacetamide [33] were reported as more in vitro cytotoxic than cisplatin.

In the present study, diiodido platinum(II) complexes *cis*-[Pt(4aza)₂I₂] (**1**), *cis*-[PtI₂(*ip*4aza)₂] (**2**), *cis*-[Pt(4aza)I₂(NH₃)] (**3**) and *cis*-[PtI₂(*ip*4aza)(NH₃)] (**4**) containing 4-azaindole (4aza) or its derivative *N*1-isopropyl-4-azaindole (1-(propan-2-yl)-1*H*-pyrrolo[3,2-*b*]pyridine; *ip*4aza) have been prepared (Fig. 1) and their purity and composition were studied by relevant techniques. Complexes **1–4** were tested for their in vitro cytotoxicity at the human ovarian carcinoma (A2780), cisplatin-resistant ovarian carcinoma (A2780R) and colon carcinoma (HT-29) cell lines. The A2780 cells were chosen for the additional studies of the crucial processes (cellular accumulation, cell cycle

Fig. 1 Synthetic pathways for the preparation of **a** *N*1-isopropyl-4-azaindole (1-(propan-2-yl)-1*H*-pyrrolo[3,2-*b*]pyridine; *ip*4aza) given with the atom numbering scheme, and **b** platinum(II) complexes *cis*-[Pt(4aza)₂I₂] (**1**), *cis*-[PtI₂(*ip*4aza)₂] (**2**), *cis*-[Pt(4aza)I₂(NH₃)] (**3**) and *cis*-[PtI₂(*ip*4aza)(NH₃)] (**4**) containing 4-azaindole (4aza) or *ip*4aza



perturbation) connected with their high antiproliferative activity at these human cancer cells.

Experimental

Materials

K_2PtCl_4 was purchased from Precious Metals Online, while other chemicals (4aza, NaH, $MgSO_4$, $AgNO_3$, KI, KCl, 2-bromopropane, NH_3 (25% water solution), HCl (35% water solution), cisplatin, reduced glutathione (GSH), L-cysteine (CysH), cytochrome c from bovine heart (Cytc), hen egg-white lysozyme (HEWL), guanosine monophosphate disodium salt hydrate (GMP), solvents (MeOH, diethyl ether (DEE), EtOH, THF, ethyl acetate, DMF, DMSO and *n*-octanol) and deuterated solvents for NMR experiments ($CDCl_3$, $DMF-d_7$, D_2O) were supplied by VWR International (Stříbrná Skalice, Czech Republic), Sigma-Aldrich (Prague, Czech Republic), Lach-Ner (Neratovice, Czech Republic) and Litolab (Chudobín, Czech Republic).

Synthesis

N1-isopropyl-4-azaindole (*ip4aza*)

NaH (1.2 mmol, 48 mg) and 4aza (1.0 mmol, 118 mg) were poured into the reaction flask, which was closed with a rubber septum and repeatedly evacuated and filled with nitrogen gas. After that, 5 mL of THF was slowly poured in to start the reaction ($-20\text{ }^\circ\text{C}$). After 15 min of stirring at $-20\text{ }^\circ\text{C}$, 2-bromopropane (1.5 mmol, 183 μL) was added to this mixture, which reacted in microwave synthesizer at $150\text{ }^\circ\text{C}$ for 1 h. After cooling to ambient temperature, the mixture was centrifuged to separate NaBr and supernatant, which was dried ($MgSO_4$), filtered, and evaporated on a rotary evaporator. The obtained brown oily product was purified using flash silica gel chromatography with the mixture of ethyl acetate and NH_3 (100:1, v/v) and using the thin-layer chromatography (TLC) control. The product (*ip4aza*; Fig. 1) was obtained as brown–yellow oil after evaporation of solvents on a rotary evaporator. ^1H NMR ($CDCl_3$, $25\text{ }^\circ\text{C}$, ppm): 8.46 (d, $J=4.4\text{ Hz}$, C5–H), 7.81 (d, $J=8.1\text{ Hz}$, C7–H), 7.55 (d, $J=2.9\text{ Hz}$, C2–H), 7.20 (dd, $J=8.4, 4.8\text{ Hz}$, C6–H), 6.83 (d, $J=2.9\text{ Hz}$, C3–H), 4.70 (sep, $J=6.6\text{ Hz}$, C8–H), 1.58 (d, $J=7.3\text{ Hz}$, C9–H₆). ^{13}C NMR ($CDCl_3$, $25\text{ }^\circ\text{C}$, ppm): 144.6 (C7a), 140.8 (C5), 129.2 (C2), 128.7 (C3a), 118.4 (C7), 115.9 (C6), 101.3 (C3), 47.9 (C8), 22.7 (C9). ^{15}N NMR ($CDCl_3$, $25\text{ }^\circ\text{C}$, ppm): 293.2 (N4), 124.9 (N1). ESI+ MS (MeOH): 161.2 (calc. 161.1 for $\{(ip4aza)+H\}^+$).

Complex *cis*-[Pt(4aza)₂I₂] (1) The solution of $K_2[PtCl_4]$ (0.2 mmol, 83 mg) in 1 mL of deionized water was heated

to $50\text{ }^\circ\text{C}$ and 5 molar equiv. of KI was added (166 mg). The reaction mixture was stirred at $50\text{ }^\circ\text{C}$ for 10 min, providing the solution of $K_2[PtI_4]$. After that, the solution was cooled to ambient temperature and the stoichiometric amount of 4aza (0.4 mmol, 47 mg) dissolved in 1 mL of MeOH was poured in. The obtained yellow suspension was stirred for 2 h, then the solid was collected by filtration and washed with water ($2\times 0.5\text{ mL}$), MeOH ($2\times 0.5\text{ mL}$), and DEE ($2\times 1\text{ mL}$). The yellow solid product was dried in desiccator under the reduced pressure (30 min) and the yield was ca. 75% (calculated to $K_2[PtCl_4]$). *Anal.* Calc. for $PtC_{14}H_{12}N_4I_2$: C, 24.5; H, 1.8; N, 8.2; Found: C, 24.9; H, 1.7; N, 8.0%. ESI+ MS (MeOH, m/z): 707.8 (calc. 708.9; 30%; $\{[Pt(4aza)_2I_2]+Na\}^+$), 675.9 (calc. 676.0; 40%; $[Pt(4aza)_3I]^+$), 558.0 (calc. 558.0; 100%; $[Pt(4aza)_2I]^+$), 430.1 (calc. 430.1; 20%; $\{[Pt(4aza)_2]-H\}^+$), 119.2 (calc. 119.0; 40%; $\{(4aza)+H\}^+$). ESI– MS (MeOH, m/z): 811.9 (calc. 811.8; 100%; $[Pt(4aza)_2I_3]^-$), 693.8 (calc. 693.7; 10%; $[Pt(4aza)_3I_2]^-$), 683.9 (calc. 683.9; 10%; $\{[Pt(4aza)_2I_2]-H\}^-$), 576.0 (calc. 575.7; 20%; $[PtI_3]^-$), 566.0 (calc. 565.8; 25%; $\{[Pt(4aza)_2]-H\}^-$). ^1H NMR ($DMF-d_7$, $25\text{ }^\circ\text{C}$, ppm): 11.89 (s, N1–H), 8.94 (d, $J=5.5\text{ Hz}$, C5–H), 7.93 (s, C2–H), 7.88 (d, $J=8.3\text{ Hz}$, C7–H), 7.52 (s, C3–H), 7.14 (s, C6–H). ^{13}C NMR ($DMF-d_7$, $25\text{ }^\circ\text{C}$, ppm): 146.4 (C7a), 144.5 (C5), 131.1 (C2), 130.6 (C3a), 121.0 (C7), 117.4 (C6), 103.6 (C3). ^{15}N NMR ($DMF-d_7$, $25\text{ }^\circ\text{C}$, ppm): 200.6 (N4), N1— not detected. ^{195}Pt NMR ($DMF-d_7$, $60\text{ }^\circ\text{C}$, ppm): -3186 . FTIR ($\nu_{ATR}\text{ cm}^{-1}$): 3284s, 3071m, 2894w, 2706w, 1569w, 1496w, 1480m, 1417vs, 1273vs, 1353s, 1327s, 1209m, 1131w, 1095w, 1059m, 888w, 792w, 760vs, 625w.

Complex *cis*-[PtI₂(*ip4aza*)₂] (2) Complex 2 was prepared by the same protocol as described for complex 1, but starting from 0.1 mmol $K_2[PtCl_4]$ and using *ip4aza* instead of 4aza. The reaction mixture was stirred for 24 h and the obtained yellow solid was collected by filtration, washed with water ($1\times 0.5\text{ mL}$), MeOH ($1\times 0.5\text{ mL}$), and DEE ($2\times 0.5\text{ mL}$), and dried in desiccator under the reduced pressure (30 min). The yield was ca. 45% (calculated to $K_2[PtCl_4]$). *Anal.* Calc. for $PtC_{20}H_{24}N_4I_2$: C, 31.2; H, 3.1; N, 7.3; Found: C, 31.3; H, 3.3; N, 7.0%. ESI+ MS (MeOH, m/z): 802.0 (calc. 802.0; 100%; $\{[Pt(ip4aza)_2I_2]+CH_3OH+H\}^+$), 791.9 (calc. 792.0; 5%; $\{[Pt(ip4aza)_2I_2]+Na\}^+$), 642.0 (calc. 642.1; 85%; $[Pt(ip4aza)_2I]^+$), 551.1 (calc. 551.1; 10%; $[Pt(ip4aza)_2Cl]^+$), 514.2 (calc. 514.2; 5%; $\{[Pt(ip4aza)_2]-H\}^+$), 161.2 (calc. 161.1; 10%; $\{(ip4aza)+H\}^+$). ESI– MS (MeOH, m/z): 735.4 (calc. 735.8; 30%; $[Pt(ip4aza)_3I_3]^-$). ^1H NMR ($DMF-d_7$, $25\text{ }^\circ\text{C}$, ppm): 8.99 (d, $J=5.9\text{ Hz}$, C5–H), 8.10 (d, $J=7.3\text{ Hz}$, C7–H), 7.54 (m, 2H, C2–H), 7.33 (bs, 2H, C3–H), 7.19 (m, 2H, C6–H), 4.83 (sep, $J=7.3\text{ Hz}$, C8–H), 1.48 (d, $J=5.8\text{ Hz}$, C9–H₆). FTIR ($\nu_{ATR}\text{ cm}^{-1}$): 3091w, 2971w, 2927w, 1608w, 1566w, 1494s, 1426vs,

1272vs, 1368 m, 1306 m, 1205 m, 1129w, 1101w, 1070w, 1014w, 792w, 760vs, 725w, 607w.

Complex *cis*-[Pt(4aza)₂(NH₃)] (3) A key intermediate K[PtI₃(NH₃)] was prepared by the modification of the formerly reported protocols [33, 34]. In particular, KI (5.4 mmol, 900 mg) was added to the solution of K₂[PtCl₄] (0.9 mmol, 375 mg) in 3 mL of distilled water at 50 °C. After 10 min of stirring at this temperature, connected with the colour change to dark red, the mixture was cooled down to the laboratory temperature and 600 μL of NH₃/water solution was added. After 30 min of stirring at ambient temperature, the yellow solid of *cis*-[PtI₂(NH₃)₂] was filtered off, washed with distilled water (1 mL), EtOH (2 × 1 mL), and DEE (2 × 1 mL), and dried under vacuum (1 h). The yield was ca. 90% (calculated to K₂[PtCl₄]).

The complex *cis*-[PtI₂(NH₃)₂] (0.82 mmol, 400 mg) was dissolved in 50 mL of distilled water at 80 °C and 2 molar equiv. of AgNO₃ (280 mg) was added. After 20 min of stirring of the reaction mixture in the dark (under aluminium foil), the formed precipitate was filtered off and the obtained filtrate was concentrated to the volume of ca. 5 mL. An excess of KCl (13.3 mmol, 990 mg) was added to the concentrated solution at 0 °C, leading to the immediate precipitation of the yellow solid of *cis*-[PtCl₂(NH₃)₂] (cisplatin), which was collected after 15 min of stirring at 0 °C. The product was washed by EtOH (3 mL) and DEE (2 × 3 mL), and dried under vacuum (1 h). The yield was ca. 60% (calculated to *cis*-[PtI₂(NH₃)₂]).

The complex *cis*-[PtCl₂(NH₃)₂] (cisplatin; 0.5 mmol, 150 mg) was suspended in 8 mL of the HCl/H₂O mixture of solvents (1:2, v/v) and heated while stirring at 120 °C for 8 h. After cooling to laboratory temperature, the unreacted cisplatin was removed by filtration and the orange filtrate was concentrated under reduced pressure. The obtained red solid was dissolved in MeOH (2 mL), filtered and solvent was removed, which was repeated three times and led to the dark red NH₄[PtCl₃(NH₃)] intermediate. NH₄[PtCl₃(NH₃)] was dissolved in 3 mL of MeOH, cooled to 0 °C and excess KOH (1.1 mmol, 60 mg) was added. The yellow solid of K[PtCl₃(NH₃)] was collected after 10 min of stirring at 0 °C, washed by EtOH (acidified by HCl; 1 mL) and DEE (2 × 1 mL), and dried under vacuum (1 h). The yield of K[PtCl₃(NH₃)] was ca. 55% (calculated to *cis*-[PtCl₂(NH₃)₂]).

The complex K[PtCl₃(NH₃)] (0.15 mmol, 54 mg) was dissolved in 1.5 mL of distilled water and KI (0.45 mmol, 75 mg) was added and the mixture was stirred at the laboratory temperature until turned red, indicating the formation of the complex K[PtI₃(NH₃)]. Then the solution of 4aza (0.30 mmol, 35 mg) in 1.5 mL of MeOH was poured in and the reaction mixture was stirred for 24 h. The resulting amber solid (complex **3**) was collected by filtration, washed

by water (1 mL), MeOH (2 × 0.5 mL) and DEE (2 × 1 mL), and dried in desiccator under the reduced pressure (2 h). The yield of the complex **3** was ca. 40% (calculated to K[PtCl₃(NH₃)]). *Anal. Calc.* for PtC₇H₉N₃I₂: C, 14.4; H, 1.6; N, 7.2; Found: C, 14.8; H, 1.6; N, 7.5%. ESI+ MS (MeOH, *m/z*): 574.9 (calc. 575.0; 5%; [Pt(NH₃)(4aza)₂I]⁺), 557.9 (calc. 558.0; 30%; [Pt(4aza)₂I]⁺), 457.0 (calc. 457.0; 10%; [Pt(NH₃)(H4aza)I]⁺), 440.0 (calc. 439.9; 15%; [Pt(4aza)I]⁺), 430.1 (calc. 430.1; 45%; {[Pt(4aza)₂]-H}⁺), 312.1 (calc. 312.0; 5%; {[Pt(4aza)-H]⁺), 119.2 (calc. 119.0; 100%; {(4aza) + H}⁺). ESI- MS (MeOH, *m/z*): 582.8 (calc. 582.9; 15%; {[Pt(NH₃)(4aza)I₂]-H}⁻), 565.9 (calc. 565.8; 35%; {[Pt(4aza)I₂]-H}⁻), 491.9 (calc. 491.9; 90%; {[Pt(NH₃)(4aza)ClI]-H}⁻), 475.0 (calc. 474.9; 50%; {[Pt(4aza)ClI]-H}⁻). ¹H NMR (DMF-*d*₇, 25 °C, ppm): 11.98 (s, N1-H), 8.62 (d, *J* = 5.1 Hz, C5-H), 8.07 (d, *J* = 8.1 Hz, C7-H), 7.97 (bs, C2-H), 7.32 (bs, C3-H), 7.25 (dd, *J* = 8.1, 5.9 Hz, C6-H), 4.33 (bs, N10-H₃). ¹³C NMR (DMF-*d*₇, 25 °C, ppm): 147.0 (C7a), 146.3 (C5), 132.0 (C2), 131.7 (C3a), 121.8 (C7), 118.3 (C6), 102.9 (C3). ¹⁵N NMR (DMF-*d*₇, 25 °C, ppm): 202.3 (N4), 135.9 (N1), -46.8 (N10-H₃). ¹⁹⁵Pt NMR (DMF-*d*₇, 60 °C, ppm): -2548. FTIR (ν_{ATR} cm⁻¹): 3559w, 3252vs, 3106, 2712w, 2598w, 1594w, 1567w, 1497s, 1417vs, 1274s, 1355w, 1326 m, 1207w, 1098w, 1060w, 889w, 762vs.

Complex *cis*-[PtI₂(*ip*4aza)(NH₃)] (4) The complex K[PtCl₃(NH₃)] (0.15 mmol, 54 mg) was dissolved in 1.2 mL of distilled water and the stoichiometric amount of KI (0.45 mmol, 75 mg) was added, providing the red solution of K[PtI₃(NH₃)]. A slight excess of *ip*4aza (0.16 mmol, 26 mg), dissolved in 1.2 mL of MeOH, was added to the water solution of K[PtI₃(NH₃)] and the mixture was stirred overnight, leading to the formation of yellow solid of complex **4**. The product was removed by filtration, washed by water (0.5 mL), MeOH (2 × 0.5 mL) and DEE (2 × 1 mL), and dried in desiccator under the reduced pressure (2 h). The yield of complex **4** was ca. 20% (calculated to K[PtCl₃(NH₃)]). *Anal. Calc.* for PtC₁₀H₁₅N₃I₂: C, 19.2; H, 2.4; N, 6.7; Found: C, 19.1; H, 2.4; N, 7.1%. ESI+ MS (MeOH, *m/z*): 659.0 (calc. 659.1; 20%; [Pt(NH₃)(*ip*4aza)₂I]⁺), 642.0 (calc. 642.1; 100%; [Pt(*ip*4aza)₂I]⁺), 531.2 (calc. 531.2; 5%; {[Pt(NH₃)(*ip*4aza)₂]-H}⁺), 514.2 (calc. 514.2; 5%; {[Pt(*ip*4aza)₂]-H}⁺), 161.2 (calc. 161.1; 30%; {(*ip*4aza) + H}⁺). ESI- MS (MeOH, *m/z*): 735.4 (calc. 735.8; 30%; [Pt(*ip*4aza)I₃]⁻), 661.9 (calc. 661.9; 30%; {[Pt(NH₃)(*ip*4aza)ClI]⁻), 570.2 (calc. 569.9; 50%; {[Pt(NH₃)(*ip*4aza)ClI]⁻). ¹H NMR (DMF-*d*₇, 25 °C, ppm): 8.64 (d, *J* = 5.1 Hz, C5-H), 8.26 (d, *J* = 8.8 Hz, C7-H), 8.11 (d, *J* = 2.9 Hz, C2-H), 7.34 (d, *J* = 2.9 Hz, C3-H), 7.28 (dd, *J* = 8.4, 5.5 Hz, C6-H), 4.95 (sep, *J* = 6.6 Hz, C8-H), 4.33 (bs, N10-H₃), 1.56 (d, *J* = 6.6 Hz, C9-H₆). FTIR (ν_{ATR} cm⁻¹): 3332 m, 3221 s, 3173 s, 3093 s, 1495 s, 2971 s, 2928 s, 2871w, 1612w,

1566w, 1495 s, 1431vs, 1302vs, 1274vs, 1205 m, 1128w, 1101w, 1067w, 1015w, 789w, 762vs, 726w.

General methods

Elemental analysis was performed by Flash 2000 CHNS Elemental Analyser (Thermo Scientific). Electrospray ionization mass spectrometry (ESI-MS; methanol solutions) was carried out with LCQ Fleet ion trap spectrometer (Thermo Scientific; QualBrowser software, version 2.0.7) in both the positive (ESI+) and negative (ESI-) ionization modes. ^1H and ^{13}C NMR spectroscopy, and ^1H - ^1H gsCOSY, ^1H - ^{13}C gsHMQC and ^1H - ^{13}C gsHMBC two dimensional correlation experiments were performed on the CDCl_3 (for *ip4aza*) or $\text{DMF-}d_7$ (complexes **1–4**) solutions at 300 K using JEOL JNM-ECA 600II spectrometer at 600.00 MHz (for ^1H NMR) and 150.9 MHz (for ^{13}C NMR); gs = gradient selected, COSY = correlation spectroscopy, HMQC = heteronuclear multiple quantum coherence, HMBC = heteronuclear multiple bond coherence. ^1H and ^{13}C NMR spectra were calibrated against the residual DMF ^1H NMR (8.03, 2.92 and 2.75 ppm) and ^{13}C NMR (163.2, 34.9 and 29.8 ppm) signals. The splitting of proton resonances in the reported ^1H spectra is defined as s = singlet, d = doublet, dd = doublet of doublets, sep = septet, m = multiplet and bs = broad signal. ^1H - ^{15}N gsHMBC experiments were carried out at natural abundance and calibrated against the residual signals of DMF adjusted to 8.03 ppm (^1H) and 104.7 (^{15}N) ppm. ^{195}Pt spectra were measured on the $\text{DMF-}d_7$ solutions and they were calibrated against $\text{K}_2[\text{PtCl}_6]$. Note: complexes **2** and **4** were characterized only by ^1H NMR, due to the low yields obtained. FTIR spectroscopy was performed using Nexus 670 FT-IR spectrometer (ThermoNicolet) at 400–4000 cm^{-1} (attenuated total reflectance (ATR) technique. Simultaneous thermogravimetry and differential scanning calorimetry (TG/DSC) were performed using TG/DSC thermal analyser STA449 F1 (Netzsch); ceramic crucible, air/He atmosphere (60/40 mL/min), from laboratory temperature to 900 °C (5.0 °C/min).

Solution behaviour

The appropriate amount of complexes **1–4** for 1 mM solutions was dissolved in 120 μL of $\text{DMF-}d_7$ and 480 μL of D_2O was added. ^1H NMR spectra were recorded at different time points over 48 h (300 K, JEOL JNM-ECA 600II). The obtained ^1H NMR spectra were calibrated against the residual signal of D_2O found at 4.85 ppm [35].

Hydrophobicity studies (logP)

Octanol-saturated water (OSW) and water-saturated octanol (WSO) were prepared from *n*-octanol and 0.2 M water

solution of KI by the overnight stirring. Stock solutions were prepared by ultrasonication (5 min) and shaking (30 min) of 1 μmol of complexes **1–4** in 20 mL of OSW. After that, the mixtures were centrifuged (5 min, 11,000 rpm) and supernatants were collected. 5 mL of this solution was added to 5 mL of WSO and shaken at ambient temperature for 2 h. After that, the mixture was centrifuged and aqueous layer was separated carefully and the Pt concentration was determined by ICP-MS (the obtained value was corrected for the adsorption effects). $\log P = \log([\text{Pt}]\text{WSO}/[\text{Pt}]\text{OSW}_a)$ equation was used for the partition coefficient calculation; $[\text{Pt}]\text{OSW}_b$ and $[\text{Pt}]\text{OSW}_a$ stands for the Pt concentration before and after partition, respectively, and $[\text{Pt}]\text{WSO} = [\text{Pt}]\text{OSW}_b - [\text{Pt}]\text{OSW}_a$.

Cell culture and cell-based studies

The human ovarian carcinoma cell line (A2780), cisplatin-resistant human ovarian carcinoma cell line (A2780R) and human colon carcinoma cell line (HT-29) were cultured according to the supplier's (European Collection of Cell Cultures, ECACC) instructions, using RPMI-1640 medium supplemented with 10% of fetal calf serum, 1% of 2 mM glutamine and 1% penicillin/streptomycin. The 96-well culture plate with the primary culture of human hepatocytes (Hep) was purchased from Biopredic Intl. and cultured according to the suppliers' instructions using the chemically defined medium consisting of a mixture of William's E and Ham's F-12 (1:1, v/v). All cell lines were grown as adherent monolayers at 37 °C and 5% CO_2 in a humidified atmosphere. The 50 mM stock solutions of complexes **1–4** were prepared by dissolving of their appropriate amount in 500 μL of DMF. Cisplatin was involved in the testing for comparative purposes.

In vitro cytotoxicity testing

The cultured A2780, A2780R, and HT-29 cells were seeded to 96-well culture plates. The A2780, A2780R, HT-29, and Hep cells were pre-incubated in drug-free media at 37 °C for 24 h and then treated for next 24 h at 37 °C with different concentrations of complexes **1–4** and cisplatin (note: only with complexes **1** and **2** for the Hep cells) prepared from their stock solutions by a dilution with the appropriate medium. After 24 h drug exposure, the supernatants were removed and the cells were washed with drug-free PBS followed by staining with MTT dye (3-(4,5-dimethylthiazol-2-yl)-2,5-diphenyltetrazolium bromide). The cell viability was determined using the spectrophotometric evaluation of the formed formazan (from MTT dye) concentration (540 nm, Infinite 200 PRO microplate reader, Tecan Group Ltd., Männedorf, Switzerland).

The data were expressed as the percentage of viability, where 100% and 0% represent the treatments with negative (0.1% DMF in medium) and positive (1% Triton X-100) controls, respectively. The data from the cancer cells were acquired from three independent experiments (conducted in triplicate) using cells from different passages. The resulting IC_{50} values (μM) were calculated from the viability curves and the results are presented as arithmetic mean \pm standard deviation (SD).

Cellular accumulation

The cultured A2780 cells were seeded in 6-well culture plates (1×10^6 cells per well) and incubated overnight (37°C and 5% CO_2 in a humidified incubator). After that the cells were treated with the IC_{50} concentrations of complexes **1–4**. The treatment was followed by washing with PBS (2×2 mL) and the washed cells were harvested by the trypsin treatment, collected and centrifuged in PBS. The supernatants were discarded after centrifugation and the obtained pellets were immediately digested in 250 μL of nitric acid (overnight, 70°C ; TMS-200 Thermo Shaker Incubator, Hangzhou Allsheng Instruments Co., Ltd., Hangzhou, China) to give the fully homogenized solutions. The solutions were diluted with 2.25 mL of water and the Pt content was determined by inductively coupled plasma mass spectrometry (ICP-MS) using the 7700 \times ICP-MS device (Agilent Technologies). The obtained values were corrected for adsorption effects. The experiments were conducted in duplicate. The untreated A2780 cells were used as a negative control and the A2780 cells treated by the IC_{50} concentration of cisplatin were involved for comparative purposes.

Cell cycle analysis

The A2780 cells (1.0×10^6 per well) were pre-incubated in a six-well plate for 24 h, as described above. Complexes **1–4** were added at their IC_{50} concentrations. After 24 h, the cells were harvested by trypsinization, washed with PBS, centrifuged and stained for 30 min by a propidium iodide (PI) supplemented with RNase A and 0.1% (v/v) Triton X-100 (25°C). After that, the DNA content was assessed using flow cytometry detecting emission at 617 nm after excitation at 535 nm (CytoFlex, Beckman Coulter). The obtained data were analysed using CytExpert™ software (Beckman Coulter). The A2780 cells treated by cisplatin (IC_{50} concentration) were involved for comparative purposes and the untreated A2780 cells were used as a negative control. All experiments were carried out in triplicate (three samples counting ca. 3×10^5 cells).

Mass spectrometry studies of interactions with sulfur-containing biomolecules and model proteins

The interactions of selected complex **2** with biomolecules (sulfur-containing agents L-cysteine (CySH) and reduced glutathione (GSH) and model proteins cytochrome c from bovine heart and hen egg-white lysozyme) were studied by means of a mass spectrometric studies involving the mixtures of complex **2** and serum levels of CySH (290 μM) and GSH (6 μM), and complex **2** and model proteins (3 mg/mL), respectively. The evaluation of the interacting species was done according to the previously published procedure [36] using a LCQ Fleet ion trap spectrometer (Thermo Scientific; QualBrowser software, version 2.0.7) in positive ionization mode (ESI+) and the spectra of mixtures containing proteins were deconvoluted using Promass for Xcalibur ver. 3.0, rev 10 software (Novatia LLC, Newtown, PA, USA) producing the neutral mass spectra, allowing us to deduce the interacting intermediates.

Statistical analysis

An ANOVA test was used for statistical analysis with the values of $p < 0.05$ (*), 0.01 (**), and 0.005 (***) considered to be statistically significant. QC Expert 3.2 Statistical software (TriloByte Ltd.) was used to perform the analysis.

Results

Chemistry

The intermediates $\text{NH}_4[\text{PtCl}_3(\text{NH}_3)]$, $\text{K}[\text{PtCl}_3(\text{NH}_3)]$, and $\text{K}[\text{PtI}_3(\text{NH}_3)]$ were prepared using the slightly modified procedures [33, 34], while the final platinum(II) complexes *cis*- $[\text{Pt}(4\text{aza})_2\text{I}_2]$ (**1**), *cis*- $[\text{PtI}_2(ip4\text{aza})_2]$ (**2**), *cis*- $[\text{Pt}(4\text{aza})\text{I}_2(\text{NH}_3)]$ (**3**) and *cis*- $[\text{PtI}_2(ip4\text{aza})(\text{NH}_3)]$ (**4**) were prepared as described in the Experimental section (Fig. 1) [37]. Complexes **1–4** were only negligibly soluble in water, methanol (MeOH), ethanol (EtOH) or acetone, but they showed good solubility in *N,N*-dimethylformamide (DMF) and dimethyl sulfoxide (DMSO). Purity of complexes **1–4** was confirmed by a combination of elemental analysis (<0.5% differences between the calculated and found percentage of C, H and N) and ^1H NMR.

ESI+ mass spectra of the *cis*- $[\text{PtI}_2(n\text{aza})_2]$ complexes **1** and **2** contained the peaks of the $\{[\text{PtI}_2(n\text{aza})_2] + \text{Na}\}^+$ and $[\text{PtI}(n\text{aza})_2]^+$ species; *naza* = 4aza or *ip4aza*. In the ESI– mass spectra, the peaks of the $[\text{Pt}(n\text{aza})\text{I}_3]^-$ species showed with appropriate *m/z* value and isotopic distribution for both complexes **1** and **2**. The peaks of several species (e.g., $\{[\text{Pt}(4\text{aza})\text{I}_2(\text{NH}_3)] - \text{H}\}^-$ for **3**), containing both

N-donor ligands (i.e., NH₃ and *naza*) were detected in the mass spectra of the sterically hindered complexes **3** and **4**.

The FTIR spectra showed the peaks of the $\nu(\text{C-H})_{\text{ar}}$ (ca. 3100 cm⁻¹), $\nu(\text{C-C})_{\text{ar}}$ (ca. 1600 cm⁻¹) and $\nu(\text{C-N})_{\text{ar}}$ (ca. 1420 cm⁻¹) vibrations of the 4-azaindole ring. In addition, the FTIR spectra of complexes **3** and **4** contained the peaks of $\nu(\text{NH}_3)$ at 3252 and 1326 cm⁻¹ (for **3**) and 3221 and 1302 cm⁻¹ (for **4**) [38]. The spectra of complexes **2** and **4** (containing *ip4aza*) showed the intensive peaks of the $\nu(\text{C-H})_{\text{aliph}}$ vibrations at 2971 and 2927 cm⁻¹ (for **2**), and at 2971 and 2928 cm⁻¹ (for **4**).

The simultaneous TG/DSC analysis proved the representative complex **1** as unsolvated and thermally stable up to ca. 110 °C. Behind this temperature, a gradual thermal decomposition was observed and finished at ca. 550 °C without the formation of thermally stable intermediates (69.2/68.0% calcd./found weight loss; calculated to PtO). The thermal decomposition was accompanied on the DSC curve by the exothermic effects centred at ca. 220, 430 and 545 °C (Fig. S1).

The ¹H NMR spectra of complexes **1–4** contained the signals of aromatic C–H hydrogen atoms at 7.14–8.94 ppm (Fig. 2, S2 and S3). In addition, the N1–H broad signal was detected in the spectra of complexes **1** and **3** containing unsubstituted 4-azaindole, while the spectra of complexes **2** and **4** (containing *ip4aza*) showed the signals of the isopropyl substituent (ca. 4.9 ppm and 1.5 ppm) of the N1 nitrogen atom. The presence of the NH₃ ligand in the structure of the sterically hindered complexes **3** and **4** was confirmed by the broad signal at 4.33 ppm (for both complexes).

The ¹³C (Fig. S4 and S5) and ¹⁵N (Fig. S6) NMR spectra were recorded only for the representative 4aza-containing complexes **1** and **3**. The individual aromatic carbon atoms of the C–H groups were clearly assigned using the ¹H–¹³C HMQC correlation experiments, while the quaternary C3a and C7a carbons were refined in the ¹H–¹³C HMBC spectra, as exemplified by the C7a (δ = 146.4 ppm for **1** and

147.0 ppm for **3**) \leftrightarrow H5 (δ = 8.94 ppm for **1** and 8.62 ppm for **3**) long-range correlation peak. The ¹⁵N NMR signal of the N4 nitrogen atom shifted considerably as a consequence of the formation of complexes **1** ($\Delta\delta$ = –92.6 ppm) and **3** ($\Delta\delta$ = –90.9 ppm), suggesting that this atom represents the coordination site of the used 4aza ligand involved in the structure of complexes **1** and **3**; $\Delta\delta = \delta_{\text{complex}} - \delta_{4\text{aza}}$. The ¹⁵N NMR signal of the NH₃ ligand showed at –46.8 ppm in the ¹H–¹⁵N HMBC spectrum of complex **3** (Fig. S6). No new signals were detected in the ¹H NMR spectra of complexes **1–4** dissolved in DMF-*d*₇ after 48 h of standing at ambient temperature, suggesting their stability in the used solvent. The ¹⁹⁵Pt NMR signals were detected at –3186 ppm for complex **1** and at –2548 ppm for complex **3** (Fig. S7).

Solution behaviour and hydrophobicity

Complexes **1** and **2** were hydrolytically stable in the 20% DMF-*d*₇/80% D₂O mixture of solvents, because no new signals showed in the obtained ¹H NMR spectra even after 72 h of standing at ambient temperature (Fig. S8); note: DMF ensured the sufficient solubility of low water soluble complexes for ¹H NMR experiments. The ¹H NMR spectra of complexes **3** and **4** showed a new set of *naza* signals (Fig. S9). For example, the representative C5–H signal was detected in the fresh solutions at 8.73 ppm (for **3**) and 8.72 ppm (for **4**), while a new C5–H signal observed during the standing of complexes **3** and **4** at 8.63 ppm (for **3**) and 8.62 ppm (for **4**). Because the C5–H signal of free H4aza showed at 8.43 ppm in the 20% DMF-*d*₇/80% D₂O mixture of solvents, the observed ¹H NMR spectral changes of complexes **3** and **4** (as discussed above) can be assigned to the hydrolysis of these complexes.

The log*P* studies were not possible to realize owing to a limited solubility of complexes **1** and **2** in the solvent system used (OSW). Complexes **3** and **4** were found to be hydrophilic with similar log*P* values (–0.78, and –0.81, respectively).

In vitro cytotoxicity and cellular accumulation

Complexes **1–4** were studied for their in vitro cytotoxicity against three human carcinoma cell lines [ovarian carcinoma (A2780), its cisplatin-resistant variant (A2780R) and colon carcinoma (HT-29)], while their cellular accumulation was studied at the representative A2780 cells only. The obtained results are summarized in Table 1 (together with cisplatin for comparative purposes).

The *cis*-[PtI₂(*naza*)₂] complexes **1** and **2** significantly (*p* < 0.005) exceeded in vitro cytotoxicity of their sterically hindered *cis*-[PtI₂(*naza*)(NH₃)] analogues **3** and **4** against the A2780 and A2780R cells. Within the pairs of the *cis*-[PtI₂(*naza*)₂] (**1** and **2**) and *cis*-[PtI₂(*naza*)(NH₃)] (**3** and **4**)

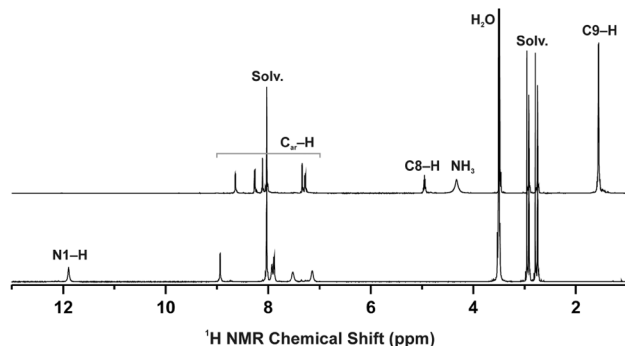


Fig. 2 ¹H NMR spectra of the representative complexes **1** (bottom) and **4** (top); DMF-*d*₇ solutions. See Fig. 1 for the structural formulas and atom numbering scheme

Table 1 The in vitro cytotoxicity ($IC_{50} \pm SD$; μM) and cellular accumulation (pmol Pt/ 10^6 A2780 cells) assessed for complexes **1–4** and cisplatin (for comparative purposes)

Complex	HT-29	A2780	A2780R	RF	Cellular accumulation
<i>cis</i> -[Pt(4aza) ₂ I ₂] (1)	4.2 ± 1.0	7.7 ± 1.2***	8.9 ± 0.1	1.2	43.0 ± 2.1
<i>cis</i> -[PtI ₂ (<i>ip</i> 4aza) ₂] (2)	4.9 ± 1.0	3.8 ± 0.8***	2.9 ± 0.3	0.8	592.3 ± 4.4
<i>cis</i> -[Pt(4aza)I ₂ (NH ₃)] (3)	5.8 ± 0.4	26.1 ± 3.0	32.4 ± 2.0	1.2	19.8 ± 0.2
<i>cis</i> -[PtI ₂ (<i>ip</i> 4aza)(NH ₃)] (4)	8.0 ± 0.6	8.9 ± 0.8***	12.1 ± 0.5	1.4	78.5 ± 3.6
Cisplatin	> 50.0	26.7 ± 1.8	> 50.0	–	86.0 ± 2.0

Cytotoxicity was studied at the human HT-29 colon carcinoma, A2780 ovarian carcinoma, and A2780R cisplatin-resistant ovarian carcinoma cells (24 h exposure time, MTT assay), with the significant differences between the obtained IC_{50} values of complexes **1–4** against cisplatin given as *** $p < 0.005$. Cellular accumulation was studied at the A2780 cells

RF resistance factor (calculated as $IC_{50}(A2780R)/IC_{50}(A2780)$)

complexes containing the same *naza* ligands, the *ip*4aza-containing complexes **2** and **4** were significantly ($p < 0.005$) more in vitro cytotoxic at the A2780 and A2780R cells than their analogues (**1** and **3**) containing the unsubstituted 4-azaindole. Complexes **1**, **2**, and **4** exhibited significantly ($p < 0.005$) higher cytotoxic potency at the A2780 cells than cisplatin. Cellular accumulation at the A2780 cells was markedly higher for (a) the *ip*4aza-containing complexes (**2**, **4**), and (b) for the complexes with two azaindoles involved in their structure (**1**, **2**), meaning that Pt of the highest-active complex **2** was accumulated significantly more than observed for other studied complexes (Table 1).

The resistance factors, calculated as $IC_{50}(A2780R)/IC_{50}(A2780)$ (see Table 1), indicated that complexes **1–4** are able to circumvent the acquired resistance of the A2780 human ovarian carcinoma cells against the therapeutic action of cisplatin.

The in vitro cytotoxicity of complexes **1–4** against the HT-29 cells ranged from the IC_{50} value of 4.2–8.0 μM , and was considerably higher as compared with cisplatin

(Table 1). Complexes **1–3** were significantly more cytotoxic ($p < 0.05$) than the least effective complex **4**. Similarly as in the A2780 cells, the *cis*-[PtI₂(*naza*)₂] complexes **1** and **2** exceeded the in vitro cytotoxicity of their ammine-containing *cis*-[PtI₂(*naza*)(NH₃)] analogues **3** and **4** at the HT-29 cells.

Complex **1** and **2** were tested for their toxicity at the primary culture of human hepatocytes (Hep). Complex **1** did not affect the viability of the Hep cells up to the highest tested concentration ($IC_{50} > 100 \mu M$), while the toxicity of complex **2** equalled $IC_{50} = 38.4 \mu M$.

Cell cycle analysis

The flow cytometry studies of the cell cycle perturbation were performed at the A2780 cells treated by the IC_{50} concentrations of complexes **1–4** and cisplatin for comparative purposes, and stained with propidium iodide (PI). The results are depicted in Fig. 3 and summarized in Table S1.

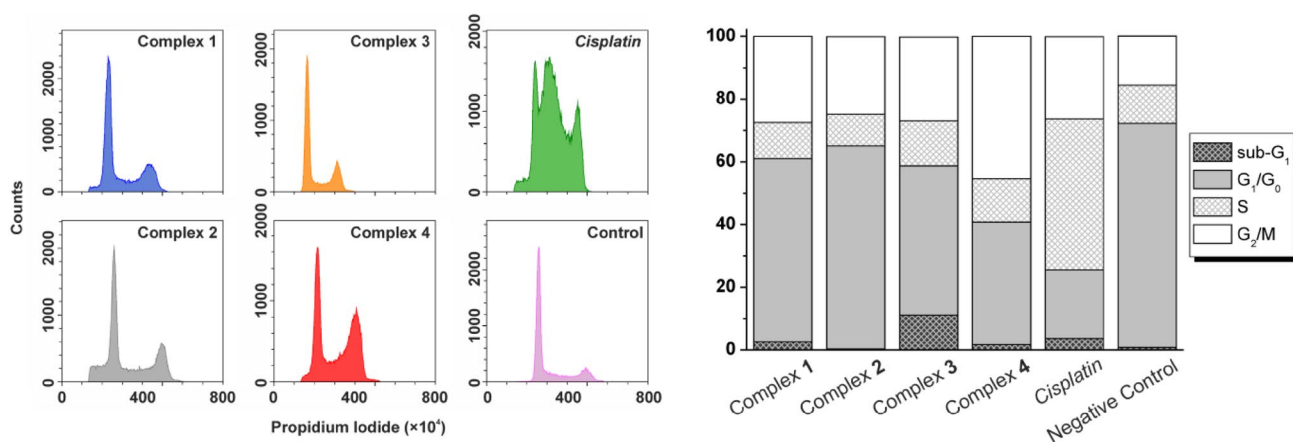


Fig. 3 Left: the selected results of the flow cytometry studies of the cell cycle modification induced at the A2780 human ovarian carcinoma cells (stained with PI/RNase) by the equitoxic (IC_{50}) concentrations of complexes **1–4** and cisplatin (for comparative purposes), given together with the negative control (untreated cells). Right:

the populations in the cell cycle phases observed at the A2780 cells treated with complexes **1–4** and cisplatin (for comparative purposes), depicted together with the negative control (untreated cells); see Table S1 for the complete data given as arithmetic mean \pm SD

The treatment of the A2780 cells by complexes **1**, **2**, and **4** induced the cell cycle perturbation connected with a decrease of the G_0/G_1 cell cycle phase population (39–58% for **1**, **2**, and **4**, and 72% for negative control) while the G_2/M cell cycle phase populations were higher for the samples treated by complexes **1**, **2**, and **4** (27–45%), as compared with the untreated cells (16%; Fig. 3 and Table S1). The most profound differences in the A2780 cell cycle were induced by the *ip4aza*-complexes **2** and **4**. Within the A2780 cells treated by complex **2**, high sub- G_1 cell cycle phase population was observed. On the other hand, the G_2/M cell cycle phase population was markedly higher for complex **4**, as compared with complexes **1–3**, as well as with conventional cisplatin. Relevant differences were also observed between the biological effect of cisplatin (48% S cell cycle phase population) and complexes **1–4** (10–14% S cell cycle phase populations).

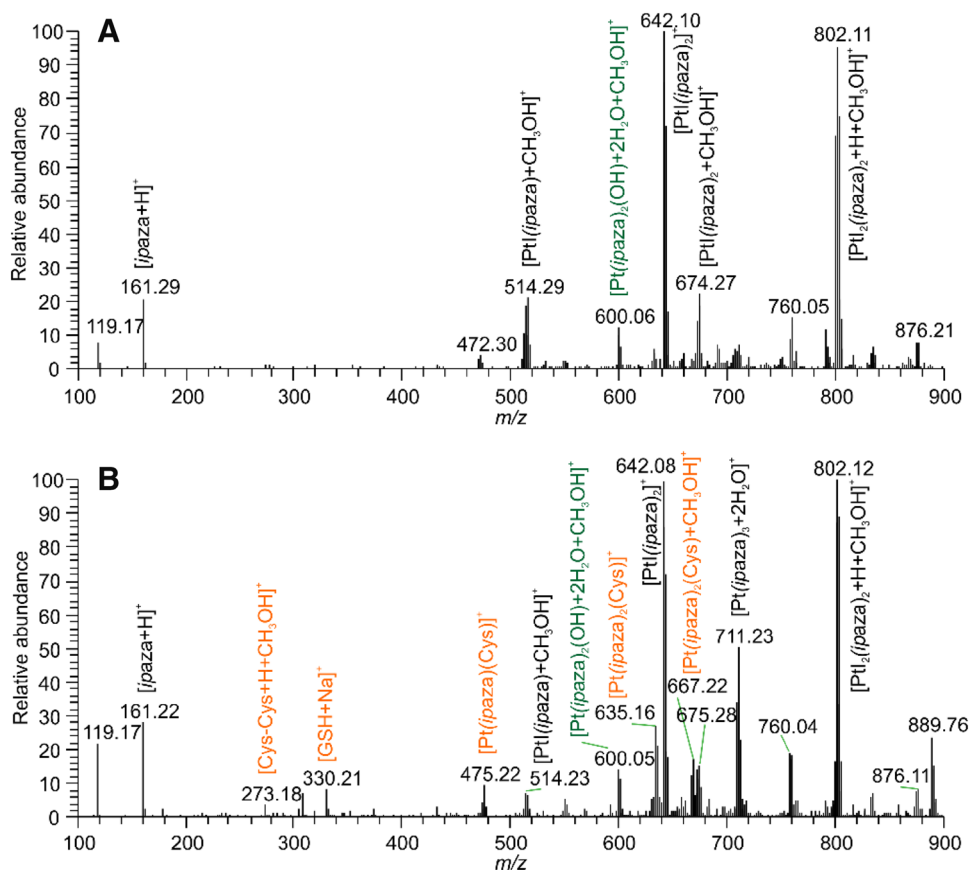
Mass spectrometry studies of interactions with sulfur-containing biomolecules and model proteins

The mass spectrometric studies revealed the moderate reactivity of the representative complex **2** with L-cysteine (CySH; a final concentration of 290 μM), as confirmed

by the appearance of the peaks in the ESI+ MS spectrum (see Fig. 4) of the mixture measured after 48 h. These signals are assignable to the species $[\text{Pt}(\text{ip4aza})(\text{Cys})]^+$ ($m/z = 475.22$), $[\text{Pt}(\text{ip4aza})_2(\text{Cys})]^+$ ($m/z = 635.16$) and $[\text{Pt}(\text{ip4aza})_2(\text{Cys}) + \text{CH}_3\text{OH}]^+$ ($m/z = 667.22$). No peaks representing the interaction species with the reduced glutathione (GSH) were found in the spectra.

Complex **2** showed higher affinity towards the cytochrome c, with whom it formed both the 1:1 and 1:2 adducts, than towards the second-used model protein HEWL (only 1:1 adduct was observed) (see Fig. 5). The mass difference in all adducts of 768 or 769 Da corresponds to the whole molar equivalent of complex **2**, which means that there can be two alternative modes of interaction of complex **2** with both proteins. The first one involves an electrostatic interaction, while the second one is associated with the formation of coordination bond between the platinum atom and appropriate donor atom from the protein, while the released iodide anion form an electrostatic interaction with positively charged surface of the protein.

Fig. 4 The ESI+ MS spectrum of the solution of complex **2** in MeOH: H₂O (1:1, v/v) after 48 h of incubation at laboratory temperature (**a**) and the ESI+ MS spectrum of the mixture containing complex **2** (at the final concentration of 10 μM), L-cysteine (at the final concentration of 290 μM) and reduced glutathione (at the final concentration of 6 μM) after 48 h of incubation at laboratory temperature (**b**). The identified species corresponding to hydrolytic intermediates are noted in green and the species corresponding to intermediates involving CySH or GSH are noted in orange colour



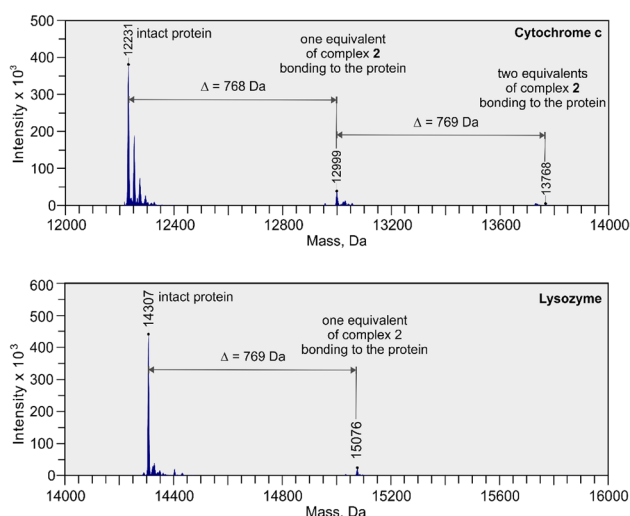


Fig. 5 The neutral mass spectra obtained by the deconvolution of the ESI+ MS spectra of the mixtures containing complex **2** (at the final concentration of 10 μ M) and one of the model proteins, cytochrome c or HEWL at the final concentration of 3 mg/mL. The depicted mass differences correspond to the formation of 1:1 and 1:2 adducts with cytochrome c (upper panel) and 1:1 adduct with lysozyme (lower panel)

Discussion

The platinum(II) complexes containing 7-azaindole and its derivatives (*7aza*) were recently reported by us and others as highly in vitro cytotoxic agents at various human cancer cell lines [11–22, 39–41]. Among these complexes of various structural types (e.g., dichlorido [13–15], diiodido [19], oxalato [17] or cyclobutane-1,1-dicarboxylato [16]) the diiodido complexes *cis*-[Pt(*7aza*)₂I₂] were the highest active ones, exceeding the cytotoxic activity of their various analogues including the dichlorido complexes and showing some pharmacological advantages over their analogues and cisplatin (e.g., different cell cycle perturbation or different interaction with relevant biomolecules). Bearing this in mind, we decided to study two structural types, *cis*-[PtI₂(*naza*)₂] (**1**, **2**) and *cis*-[PtI₂(*naza*)(NH₃)] (**3**, **4**), of platinum(II) diiodido complexes containing 4-azaindole (*4aza*) or its N1-alkylated derivative *ip4aza*. Design of this series of compounds allowed us to evaluate, whether (a) the platinum(II) complexes containing 4-azaindoles show the in vitro cytotoxicity against the selected human cancer cell lines, as recently reported for similar complexes with 7-azaindoles, (b) the replacement of the NH₃ ligand by *naza* affects the in vitro cytotoxicity of the studied complexes, and (c) the N1-alkylation of the 4-azaindole moiety affects the in vitro cytotoxicity of complexes containing such ligands.

A series of four diiodido platinum(II) complexes of the general formulas *cis*-[PtI₂(*naza*)₂] (**1**, **2**) and *cis*-[PtI₂(*naza*)(NH₃)] (**3**, **4**) (Fig. 1) was prepared and thoroughly

characterized. The syntheses of complexes **1** and **2** started from K₂[PtCl₄] through the key intermediate K₂[PtI₄] [37], whose stoichiometric reaction with *4aza* and *ip4aza* led to complexes **1** and **2**, respectively, as described for example for similar diiodido platinum(II) complexes containing 7-azaindole and its various *C*-derivatives [19]. The syntheses of complexes **3** and **4** also started from K₂[PtCl₄] and they were conducted through the *cis*-[PtCl₂(NH₃)₂] (cisplatin), NH₄[PtCl₃(NH₃)], K[PtCl₃(NH₃)] and K[PtI₃(NH₃)] intermediates, similarly as described previously [33, 34]. Finally, the reactions of K[PtI₃(NH₃)] with either *4aza* or *ip4aza* provided complexes **3** and **4**, respectively (Fig. 1).

Concerning the ¹H NMR spectroscopy, the preparation of *ip4aza* led to the disappearance of the N1–H signal of *4aza* (due to deprotonation) and detection of two new signals at 4.70 ppm and 1.58 ppm (due to alkylation), clearly assignable to the isopropyl substituent of *ip4aza* [42]. Similar differences were observed also for the pairs of the *cis*-[PtI₂(*naza*)₂] (**1** and **2**) and *cis*-[PtI₂(*naza*)(NH₃)] (**3** and **4**) complexes containing *4aza* (for **1** and **3**) or *ip4aza* (for **2** and **4**) ligands. The NH₃ ligand of complexes **3** and **4** showed for both complexes at 4.33 ppm, which is consistent with similar complexes of the *cis*-[PtI₂(L)(NH₃)] type, where L stands for pyrimidine or 5,7-diphenyl-1,2,4-triazolo[1,5-*a*]pyrimidine (L¹) [32, 43]. The positions of the ¹⁹⁵Pt NMR signals in the spectra of complexes **1** and **3** (Fig. S6) correlated well with the formerly reported complexes *cis*-[PtI₂(L¹)₂] and *cis*-[PtI₂(L¹)(NH₃)] containing 5,7-diphenyl-1,2,4-triazolo[1,5-*a*]pyrimidine (L¹) [32].

The *cis*-[PtI₂(*naza*)₂] complexes **1** and **2** are hydrolytically stable in 20% DMF-*d*₇/80% D₂O, while the sterically hindered complexes **3** and **4** hydrolysed under the used experimental conditions. Hydrolysis of complexes **3** and **4** is not connected with a release of the *naza* ligand, because the positions of the ¹H NMR signals were different for the new signals in the spectra of complexes **3** and **4**, and free *naza*. In general, hydrolytic stability of platinum(II) diiodido complexes depends on the *N*-donor ligand involved in their structures. In particular, the *cis*-[PtI₂(NH₃)₂] complex, an iodido analogue of cisplatin, readily hydrolysed at physiological pH which was connected with a release of both the halogenido ligands (similarly as for cisplatin) [44]. The hydrolysis rate was somehow slower for *cis*-[PtI₂(NH₃)₂] as compared with cisplatin. However, a release of the NH₃ ligand at slightly acidic pH was also observed in the same work for *cis*-[PtI₂(NH₃)₂], indicating its different solution behaviour from cisplatin. The *cis*-[Pt(*7aza*¹)₂I₂] complex (*7aza*¹ = 4-bromo-7-azaindole), representing platinum(II) diiodido complexes containing 7-azaindoles, showed high hydrolytic stability, because only ca. 10% hydrolysed in the used 10% DMF-*d*₇/90% D₂O mixture of solvents after 48 h of standing at ambient temperature [19]. Concerning the hydrolysis of complex **2**, the ESI+ MS studies uncovered

only the formation of a deiodinated hydroxido-intermediate with the proposed composition $[\text{Pt}(\text{ip4aza})_2(\text{OH}) + 2\text{H}_2\text{O} + \text{CH}_3\text{OH}]^+$ after 48 h of incubation.

On the other hand, the interaction studies involving sulfur-containing biomolecules, L-cysteine and reduced glutathione confirmed the moderate reactivity of complex **2** towards the normal serum levels of L-cysteine, as demonstrated by the emergence of new peaks in the ESI+ MS spectrum (see Fig. 4). Moreover, the interaction studies involving the model proteins cytochrome c and lysozyme (see Fig. 5) revealed the ability of complex **2** to form the adduct containing up to 2 molecules of complex **2** per one molecule of cytochrome c and the formation of 1:1 adduct with lysozyme. This finding may indicate that the nature of the interaction between complex **2** and model proteins could involve either pure electrostatic interaction or the covalent bonding of the deiodinated species accompanied at the same time by the electrostatic interaction of the released iodide anions with cationic parts of the protein.

The in vitro cytotoxicity of complexes **1–4** was screened at three human cancer cell lines, carefully chosen to represent the cisplatin-sensitive cells (A2780), cells with acquired resistance to cisplatin (A2780R) and cells known to be intrinsically resistant to cisplatin (HT-29) (Table 1). Complex **2** was significantly ($p < 0.01$) more cytotoxic than complex **1**, and complex **4** exceeded significant ($p < 0.005$) potency of complex **3** against the A2780 cells. Similarly, the ip4aza-containing complexes **2** and **4** exceeded the cytotoxic activity of their 4aza-containing analogues **1** and **3**, respectively, at the A2780R cells. This suggests that alkylation of 4-azaindole moiety affected the in vitro cytotoxicity of both types of the studied complexes in a positive way at both the cisplatin-sensitive and -resistant human ovarian carcinoma cells (i.e., A2780, A2780R). Further, the results also proved that complexes **1** and **2** are more in vitro cytotoxic than their sterically hindered analogues **3** and **4** against the A2780 and A2780R cells, indicating that the replacement of the NH_3 ligand by naza has a positive impact on the resulting cytotoxic potency. The opposite trend was reported for a pair of the $\text{cis-}[\text{PtI}_2(\text{L}^1)_2]$ ($\text{IC}_{50} = 67 \mu\text{M}$) and $\text{cis-}[\text{PtI}_2(\text{L}^1)(\text{NH}_3)]$ ($\text{IC}_{50} = 7 \mu\text{M}$) complexes studied at the A549 non-small lung carcinoma cells [32].

Concerning a comparison with other platinum(II) iodido complexes studied at the human ovarian carcinoma cells, the relative activity (RA; see Introduction) of the best-performing complex **2** equalled ca. 7.0, meaning approximately 7-fold higher cytotoxicity as compared with cisplatin at the used A2780 cells. The $\text{cis-}[\text{PtI}_2(\text{ipam})_2]$ complex, where ipam stands for isopropylamine, was studied at several human cancer cell lines including the A2780 cells, where this agent markedly exceeded cisplatin (RA ~ 7.3; sulforhodamide B (SRB) assay, 48 h exposure time) [45]. The complex $\text{cis-}[\text{PtI}_2(\text{NH}_3)_2]$, an iodido

analogue of cisplatin, had RA ~ 3.4 against the IGROV-1 ovarian carcinoma cells (Trypan blue assay, 24 h exposure) [44], while the complex $\text{cis-}[\text{Pt}(7\text{aza}^2)_2\text{I}_2]$ showed RA ~ 16.5 against the A2780 cells ($7\text{aza}^2 = 2\text{-methyl-4-chloro-7-azaindole}$; MTT assay, 24 h exposure time) [19]. The complex $\text{cis-}[\text{PtI}_2(\text{L}^2)(\text{NH}_3)]$ exhibited ca. 2-fold lower activity (RA ~ 0.5) at the A2780 cells than cisplatin (MTT assay, 72 h exposure time) [33].

Similar cytotoxicity of complexes **1–4** at both the A2780 and A2780R cells resulted in the resistance factors (RF) of ca. 0.8–1.4 (Table 1), indicating their ability to overcome the acquired resistance of the human cancer cells against cisplatin. This has to be highlighted especially for the best-performing complex **2** showing unusually low RF ~ 0.8. The complex $\text{cis-}[\text{Pt}(7\text{aza}^2)_2\text{I}_2]$, containing 7-azaindole-based N-donor ligand, was also somehow more in vitro cytotoxic at the resistant variant ($\text{IC}_{50} = 1.0 \mu\text{M}$) than at the cisplatin-sensitive A2780 cells ($\text{IC}_{50} = 1.7 \mu\text{M}$), meaning that RF was ca. 0.6 [19]. Similar trend of in vitro cytotoxicity (RF = 0.8) was also reported for the above-mentioned sterically hindered complex $\text{cis-}[\text{PtI}_2(\text{L}^2)(\text{NH}_3)]$ [33].

Complexes **1**, **2**, and **4** exhibited comparable in vitro cytotoxicity against the cisplatin-resistant HT-29 and cisplatin-sensitive A2780 cells, while complex **3** was markedly more potent at the HT-29 cells than at the A2780 ones (Table 1). All complexes **1–4** were considerably more cytotoxic at the HT-29 cells than cisplatin. Although the RA values could not be calculated, it can be stated that complexes **1** and **2** are more than 10-times more cytotoxic at the HT-29 colon carcinoma cells than cisplatin. The RA value of the complexes $\text{cis-}[\text{PtI}_2(\text{NH}_3)_2]$ and $[\text{Pt}(\text{dach})\text{I}_2]$ equalled ca. 1.4 and 0.6 at the HT-29 cells (Trypan blue assay, 24 h exposure; dach = (1*R*,2*R*)-cyclohexane-1,2-diamine) [46]. A representative of the platinum(II) diiodido complexes containing 7-azaindoles, $\text{cis-}[\text{Pt}(7\text{aza}^2)_2\text{I}_2]$, was several times more in vitro cytotoxic ($\text{IC}_{50} = 0.4 \mu\text{M}$) than cisplatin ($\text{IC}_{50} > 90 \mu\text{M}$) at the Caco-2 human colon carcinoma cells (MTT assay, 24 h exposure time) [19]. Further, the complex $\text{trans-}[\text{Pt}(\text{ach})\text{I}_2(\text{L}^3)]$ showed higher activity ($\text{IC}_{50} = 1.5 \mu\text{M}$) against the HT-29 cells than cisplatin ($\text{IC}_{50} > 100 \mu\text{M}$; 72 h exposure, MTT assay); ach = cyclohexanamine, $\text{L}^3 = 1,3\text{-dimethyl-}N\text{-boc-}O\text{-methylhistidin-2-ylidene}$ [47].

Complexes **1** and **2** showed a pharmacologically prospective selectivity towards the cancer cells over the non-cancerous ones. In particular, toxicity of the best-performing complex **2** was approximately one order of magnitude lower at the primary culture of human hepatocytes than at the used cancer cells. Although these results indicated higher toxicity of complex **2** than determined for cisplatin under the same experimental conditions ($\text{IC}_{50} > 75 \mu\text{M}$), it has to be highlighted that both complexes **1** and **2** are much less effective against the Hep cells than their recently reported analogues containing 7-azaindole-based ligands, which showed the

IC₅₀ values of 3.8–11.8 μM at the Hep cells (MTT assay, 24 h exposure time) [19].

The studies of cellular accumulation by the A2780 cells showed good correlation between cytotoxicity and amount of platinum uptaken by the used cells (Table 1). In particular, the best-performing complex **2** was markedly (one order of magnitude) more accumulated by the used cells than complexes **1**, **3**, and **4**, as well as than cisplatin. It is also noteworthy that complex **4** and cisplatin showed different cytotoxicity while their cellular accumulation was comparable, and on the other hand, complex **3** and cisplatin showed different cellular accumulation while their potency at the A2780 cells was of the same level. On the other hand, the correlation of cellular accumulation and log*P* (or cytotoxicity and log*P*) is not possible, because both the complexes are comparably hydrophilic, but their cellular accumulation and cytotoxicity differ markedly.

The cytotoxic effect of complexes **1**, **2**, and **4** at the A2780 cells was connected with the profound cell cycle changes, as compared with the results obtained by the analogical experiments for the untreated cells (negative control) as well as for the cells treated by the equipotent concentration of cisplatin, implying different mechanism of action of these diiodido platinum(II) complexes and cisplatin (Fig. 3 and Table S1). However, the relevant differences were observed also in the individual cell cycle phase populations of the *ip*4aza-containing complexes **2** (high sub-G₁ population) and **4** (high G₂/M population). This indicates that the structural type of the studied complexes could be decisive for the cell cycle progress of the cells treated by such complexes. Importantly, the cell cycle perturbation induced by complexes **1**, **2**, and **4** at the A2780 cells was different than in the case of the platinum(II) diiodido complexes containing 7-azaindoles [19], 9-deazahypoxanthine derivatives [48] or sterically hindered complexes containing 1-(cyclohexylmethyl)-3-methylimidazol-2-ylidene and G-quadruplex-binding pyridodicarboxamide [49], which, similarly to the herein studied complex **3**, did not modify the cell cycle of the A2780 human cancer cells.

Conclusions

In the present work, we synthesized four new *cis*-diiodido-platinum(II) complexes of two structural types, either containing two 4-azaindole-based ligands (complexes **1** and **2**) or ammine complexes with only one 4-azaindole-based ligand (complexes **3** and **4**). The *in vitro* cytotoxicity of complexes **1–4** was investigated at three cell lines with different sensitivity towards cisplatin (A2780, A2780R, and HT-29). Besides high *in vitro* cytotoxicity (IC₅₀ ≈ 3–9 μM) of the studied complexes **1** and **2** containing 4-azaindole-based ligands, their low toxicity at non-cancerous cells [primary

culture of human hepatocytes (Hep) was used; IC₅₀ > 100 μM (**1**) and IC₅₀ = 38 μM (**2**)] has to be pointed out as a significant improvement from the recently reported analogues containing various 7-azaindole derivatives (toxicity at Hep cells with IC₅₀ ≈ 4–12 μM). The obtained results indicated that 4-azaindole and its derivatives have to be taken into account as suitable ligands for development of prospective platinum anticancer complexes, because complexes **1–4** exceeded the cytotoxicity of conventional cisplatin at the used human cancer cells. Further, the alkylation of 4-azaindole moiety as well as the replacement of the NH₃ ligand by 4-azaindole-based ligand had a positive effect on the *in vitro* cytotoxicity and cellular accumulation within a series of the studied complexes.

Acknowledgements The authors gratefully thank the National Program of Sustainability I (LO1305) of the Ministry of Education, Youth and Sports of the Czech Republic and Palacký University in Olomouc (a Grant No. PrF_2018_011) for financial support. The authors also thank Ms. Kateřina Kubešová and Ms. Marta Rešová for performing the *in vitro* cytotoxicity experiments and preparation of the samples for cellular accumulation and flow cytometry experiments, Dr. Bohuslav Drahoš for recording the ESI–MS and NMR spectra, Dr. Alena Klaničková for performing FTIR spectroscopy and Mrs. Pavla Richterová for carrying out elemental analyses. The authors also thank Mr. Ivan Saksa for his help with the syntheses of the studied compounds.

References

- Kelland L (2007) *Nat Rev Cancer* 7:573–584
- Rosenberg B, van Camp L, Krigas T (1965) *Nature* 205:698–699
- World Health Organization (2017) WHO model list of essential medicines. WHO, Geneva
- Johnstone TC, Suntharalingam K, Lippard SJ (2016) *Chem Rev* 116:3436–3486
- Park GA, Wilson JJ, Song Y, Lippard SJ (2012) *Proc Natl Acad Sci USA* 109:11987–11992
- Li JJ, Tian M, Tian Z, Zhang S, Yan C, Shao C, Liu Z (2018) *Inorg Chem* 57:1705–1716
- Yang GJ, Zhong HJ, Ko CN, Wong SY, Vellaisamy K, Ye M, Ma DL, Leung CH (2018) *Chem Commun* 54:2463–2466
- Štarha P, Trávníček Z, Dvořák Z (2018) *Chem Commun* 54:9533–9536
- Mukherjee N, Podder S, Mitra K, Majumdar S, Nandi D, Chakravarty AR (2018) *Dalton Trans* 47:823–835
- Zhao SB, Wang S (2010) *Chem Soc Rev* 39:3142–3156
- Harrison RC, McAuliffe CA, Friedman ME (1984) *Inorg Chim Acta* 92:43–46
- Štarha P, Marek J, Trávníček Z (2012) *Polyhedron* 33:404–409
- Štarha P, Trávníček Z, Popa A, Popa I, Muchová T, Brabec V (2012) *J Inorg Biochem* 115:57–63
- New EJ, Roche C, Madawala R, Zhang JZ, Hambley TW (2009) *J Inorg Biochem* 103:1120–1125
- Pracharova J, Saltarella T, Radosova Muchova T, Scintilla S, Novohradsky V, Novakova O, Intini FP, Pacifico C, Natile G, Ilik P, Brabec V, Kasparkova J (2015) *J Med Chem* 58:847–859
- Štarha P, Trávníček Z, Dvořák Z, Radošová-Muchová T, Prachařová J, Vančo J, Kašpárková J (2015) *PLoS One* 10:e0123595

17. Štarha P, Trávníček Z, Popa I, Dvořák Z (2014) *Molecules* 19:10832–10844
18. Štarha P, Trávníček Z, Pazderová L, Dvořák Z (2016) *J Inorg Biochem* 162:109–116
19. Štarha P, Vančo J, Trávníček Z, Hošek J, Klusáková J, Dvořák Z (2016) *PLoS One* 11:e0165062
20. Štarha P, Hošek J, Vančo J, Dvořák Z, Suchý P Jr, Popa I, Pražanová G, Trávníček Z (2014) *PLoS One* 9:e90341
21. Štarha P, Dvořák Z, Trávníček Z (2015) *PLoS One* 10:e0136338
22. Muchová T, Prachařová J, Štarha P, Olivová R, Vrána O, Benešová B, Kašpárková J, Trávníček Z, Brabec V (2013) *J Biol Inorg Chem* 18:579–589
23. Štarha P, Vančo J, Trávníček Z (2019) *Coord Chem Rev* 380:103–135
24. Messori L, Cubo L, Gabbiani C, Alvarez-Valdes A, Michelucci E, Pieraccini G, Rios-Luci C, Leon LG, Padron JM, Navarro-Ranninger C, Casini A, Quiroga AG (2012) *Inorg Chem* 51:1717–1726
25. Sá DS, Fernandes AF, Silva CDS, Costa PPC, Fonteles MC, Nascimento NRF, Lopes LGF, Sousa EHS (2015) *Dalton Trans* 44:13633–13640
26. Przyojski JA, Kiewit ML, Fillman KL, Arman HD, Tonzetich ZJ (2015) *Inorg Chem* 54:9637–9645
27. Chatterji M, Shandil R, Manjunatha MR, Solapure S, Ramachandran V, Kumar N, Saralaya R, Panduga V, Reddy J, Prabhakar KR, Sharma S, Sadler C, Cooper CB, Mdluli K, Iyer PS, Narayanan S, Shirude PS (2014) *Antimicrob Agents Chemother* 58:5325–5331
28. Shirude PS, Shandil RK, Manjunatha MR, Sadler C, Panda M, Panduga V, Reddy J, Saralaya R, Nanduri R, Ambady A, Ravishankar S, Sambandamurthy VK, Humnabadkar V, Jena LK, Suresh RS, Srivastava A, Prabhakar KR, Whiteaker J, McLaughlin RE, Sharma S, Cooper CB, Mdluli K, Butler S, Iyer PS, Narayanan S, Chatterji M (2014) *J Med Chem* 57:5728–5737
29. Lee W, Crawford JJ, Aliagas I, Murray LJ, Tay S, Wang WR, Heise CE, Hoeflich KP, La H, Mathieu S, Mintzer R, Ramaswamy S, Rouge L, Rudolph J (2016) *Bioorg Med Chem Lett* 26:3518–3524
30. Wang T, Yang Z, Zhang ZX, Gong YF, Riccardi KA, Lin PF, Parker DD, Rahematpura S, Mathew M, Zheng M, Meanwell NA, Kadow JF, Bender JA (2013) *Bioorg Med Chem Lett* 23:213–217
31. Pin F, Buron F, Saab F, Colliandre L, Bourg S, Schoentgen F, Le Guevel R, Guillouzo C, Routier S (2011) *Med Chem Commun* 2:899–903
32. Łakomska I, Fandzloch M, Popławska B, Sitkowski J (2012) *Spectrochim Acta A* 91:126–129
33. Margiotta N, Denora N, Ostuni R, Laquintana V, Anderson A, Johnson SW, Trapani G, Natile G (2010) *J Med Chem* 53:5144–5154
34. Battle AR, Choi R, Hibbs DE, Hambley TW (2006) *Inorg Chem* 45:6317–6322
35. Gottlieb HE, Kotlyar V, Nudelman A (1997) *J Org Chem* 62:7512–7515
36. Massoud SS, Louka FR, Ducharme GT, Fischer RC, Mautner FA, Vančo J, Herchel R, Dvořák Z, Trávníček Z (2018) *J Inorg Biochem* 180:39–46
37. Rochon FD, Buculei V (2004) *Inorg Chim Acta* 357:2218–2230
38. Malik M, Wysokiński R, Zierkiewicz W, Helios K, Michalska D (2014) *J Phys Chem A* 118:6922–6934
39. Ruiz J, Rodríguez V, de Haro C, Espinosa A, Pérez J, Janiak C (2010) *Dalton Trans* 39:3290–3301
40. Zamora A, Rodríguez V, Cutillas N, Yellol GS, Espinosa A, Samper KG, Capdevila M, Palacios Ó, Ruiz J (2013) *J Inorg Biochem* 128:48–56
41. Pracharova J, Radosova Muchova T, Dvorak Tomastikova E, Intini FP, Pacifico C, Natile G, Kasparkova J, Brabec V (2016) *Dalton Trans* 45:13179–13186
42. Colley HE, Muthana M, Danson SJ, Jackson LV, Brett ML, Harrison J, Coole SF, Mason DP, Jennings LR, Wong M, Tulasi V, Norman D, Lockey PM, Williams L, Dossetter AG, Griffen EJ, Thompson MJ (2015) *J Med Chem* 58:9309–9333
43. Rochon FD, Titouna H (2010) *Inorg Chim Acta* 363:1679–1693
44. Marzo T, Pillozzi S, Hrabina O, Kasparkova J, Brabec V, Arcangeli A, Bartoli G, Severi M, Lunghi A, Totti F, Gabbiani C, Quiroga AG, Messori L (2015) *Dalton Trans* 44:14896–14905
45. Messori L, Casini A, Gabbiani C, Michelucci E, Cubo L, Rios-Luci C, Padron JM, Navarro-Ranninger C, Quiroga AG (2010) *ACS Med Chem Lett* 1:381–385
46. Cirri D, Pillozzi S, Gabbiani C, Tricomi J, Bartoli G, Stefanini M, Michelucci E, Arcangeli A, Messori L, Marzo T (2017) *Dalton Trans* 46:3311–3317
47. Schmitt F, Donnelly K, Muenzner JK, Rehm T, Novohradsky V, Brabec V, Kasparkova J, Albrecht M, Schobert R, Mueller T (2016) *J Inorg Biochem* 163:221–228
48. Vančo J, Trávníček Z, Křikavová R, Gálíková J, Chalupová M, Dvořák Z (2017) *J Photochem Photobiol B Biol* 173:423–433
49. Betzer JF, Nuter F, Chtchigrovsky M, Hamon F, Kellermann G, Ali S, Calmégane MA, Roque S, Poupon J, Cresteil T, Teulade-Fichou MP, Marinetti A, Bombard S (2016) *Bioconj Chem* 27:1456–1470

Publisher's Note Springer Nature remains neutral with regard to jurisdictional claims in published maps and institutional affiliations.